Research Article Open Access

Athos Agapiou*, Nikos Papadopoulos, and Apostolos Sarris

Detection of olive oil mill waste (OOMW) disposal areas using high resolution GeoEye's OrbView-3 and Google Earth images

DOI 10.1515/geo-2016-0067
Received Sep 17, 2015; accepted Apr 13, 2016

Abstract: The olive oil industry is considered to be as one of the driving sectors of the agricultural economy of the Mediterranean basin. The extraction of olive oil generates huge quantities of wastes that may have a great impact on land and water environments due to high concentrations in phenolic compounds that could cause ophytotoxicity. This paper aims to examine the potential use of freely distributed satellite images for the detection of olive oil mil waste (OOMW) areas in the island of Crete through the use of two cases studies. In the first case study an archive GeoEye OrbView-3 image was used to detect OOMW areas using the Spectral Angle Mapper detection algorithm and other geometric and topographic parameters. In the second case study, Google Earth images were examined through different classification algorithms at different scales. The overall results demonstrate that remote sensing techniques can be used as an alternative to field observations so as to detect and monitor OOMW areas Furthermore, freely distributed RGB images from digital globes (such as Google Earth) can be sufficiently and effectively used for this purpose.

Keywords: olive mill waste water; disposal areas; GeoEye OrbView-3; Google Earth; classification

***Corresponding Author: Athos Agapiou:** Department of Civil Engineering and Geomatics, Faculty of Engineering and Technology, Cyprus University of Technology, 2-6, Saripolou Str., 3603, Limassol, Cyprus; Laboratory of Geophysical-Satellite Remote Sensing & Archaeo-environment, Institute for Mediterranean Studies, Foundation for Research & Technology, Hellas (F.O.R.T.H.); Email: athos.agapiou@cut.ac.cy; Tel.: +357-25-002471; Fax: +357-25-002 769
Nikos Papadopoulos: Laboratory of Geophysical-Satellite Remote Sensing & Archaeo-environment, Institute for Mediterranean Studies, Foundation for Research & Technology, Hellas (F.O.R.T.H.); author contributed equally to this work; Email: nikos@ims.forth.gr
Apostolos Sarris: Laboratory of Geophysical-Satellite Remote Sensing & Archaeo-environment, Institute for Mediterranean Studies, Foundation for Research & Technology, Hellas (F.O.R.T.H.); author contributed equally to this work; Email: asaris@ret.forthnet.gr

1 Introduction

There are approximately 750 million productive olive trees worldwide, 98% of them located around the Mediterranean region, where more than 97% of the world's olive oil is produced. Based on Food and Agricultural Organization statistics, more than 3,269,248 tons of olive oil have been produced worldwide during 2014. The three major olive oil producers worldwide are Spain, Italy, and Greece [1, 2]. Olive oil industry is very important in Mediterranean countries, both in terms of wealth and tradition and is considered to be as one of the driving sectors of the agricultural economy of the Mediterranean basin.

Nevertheless, the extraction of olive oil generates huge quantities of wastes that have a great impact on land and water environments due to high phytotoxicity. The olive husk and wastewater produced from oil extraction processes contain macromolecules such as polysaccharides, lipids, proteins and a number of monocyclic and polymeric aromatic molecules generally known as phenolic compounds. The levels of phenols in wastewater and olive husk can vary from 1 to 8 g/l and from 2.9 to 3.7 mg/g, respectively [3]. Olive Oil Mills' Wastes (OOMW), which have dark brown color with unpleasant smell, consist mainly of water, high organic (mainly phenols and polyphenols) and low inorganic compounds (*e.g.* potassium and phosphorus), as well as grease. They are also characterized by low resistivity (0.7-5 Ohm-m), acid PH (4.0-5.5), increased Biochemically Oxygen Demand (40-95 g/l) and Chemically Oxygen Demand (50-180 g/l) values and their toxicity is mainly dependent on their high concentration of phenolic compounds [4].

Several studies have shown the negative effects of these wastes on soil microbial populations [5] or on aquatic ecosystems [6]. Inappropriate disposal of olive husk and olive mill wastewater create environmental problems such as odor and ammonia released into the atmosphere and leaching of inorganic and organic substances to the soil as well as leaching of these pollutants into the ground water [3]. The introduction of olive solid and liquid waste into soil tends to increase the average diameter of the soil aggregates, bulk density and slows down hydraulic conductivity. Polyphenols are well known to affect nitrification in the soil and have deleterious effect on soil microbial activity. The high C:N ratio and low pH are also known to immobilize nitrogen in the soil [3].

In addition to solid waste generated in the olive groves by annual pruning of olive trees, a significant amount of solid waste is generated during milling in the form of leaves and small twigs brought to the mill with the olives and in the form of crushed olive seeds and sizeable remnants of olive pulp following olive oil extraction. Leaves and twigs can be used as animal feed or in the production of compost after mixing with other appropriate materials [7]. OOMW liquid waste is also produced when substantial amounts of water are added during olive milling and olive oil extraction. From an environmental point of view, OOMW is the most hazardous in terms of the environmental impact waste produced by olive-mills in terms of quantity as well as quality. Sixty-five (65Kg) to one hundred seventy-five (175 kg) of residue liquid may be extracted from 100 kg of olives [8, 9].

Pollution from olive oil production is often a problem in economically disadvantaged communities where sophisticated solutions to the problem are too expensive [6]. The OOMW uncontrolled disposal areas in aquatic and terrestrial receptors are associated with detrimental effects because of their high content in salts and in organic matter. As a consequence, OOMW can inhibit plant and microbial growth, alter soil fungal and bacterial communities' structure as well as soil physicochemical properties [10]. OOMW are difficult to monitor due to their seasonal occurrence as well their high geographical distribution. In order to avoid environmental impacts such as soil and air pollution, olive mills are forced to treat or eliminate this OMWW using a variety of techniques and technologies. Therefore, current research efforts have been oriented towards the development of efficient treatment technologies, namely physical, chemical and biological processes as well as various combinations of them [1].

The systematic monitoring of OOMW disposal areas is therefore of great importance from an ecological perspective. However, such areas are only detected and monitored from field observations and recordings. OMWW disposal areas are generally scattered in different places with diverse local topographical and geological settings, while their identification might be difficult and time consuming if based purely on in-situ observations. The authors have recently recorded more than 1000 OOMW disposal areas in the island of Crete based on Global Navigation Satellite Systems (GNSS) and Geographical Information Systems (GIS) [11]. Additional time lapse monitoring of the wastes' flow into the subsurface has been made through ground remote sensing techniques based on electrical resistivity tomography and coring sampling [12].

Remote sensing images can provide a systematic and cost-effective methodology for large spatial scale surveys [13] and therefore assist local authorities to identify the position of illegal OOMW sites. In the literature, only a limited number of publications exist related to this topic [14–16]. This relative low number of publications should be linked to the local problem of OOMW disposal areas in the Mediterranean countries. Similar studies related either to the detection of uncontrolled landfills or to hazardous wastes [17–21] have shown the great potential of remote sensing to detect these sites. The synoptic view of overhead remote imaging can be very useful for the recognition and remediation of landfills and waste disposal areas.

A recent study [14] has shown that very high resolution IKONOS data proved to be particularly effective for the quantification of OOMW ponds in the island of Crete. In contrast, the same study indicated that free distributed medium resolution Landsat 8 OLI images can be problematic for the detection of OOMW areas since they provide controversial results. Spectral regions and OOMW index suitable to enhance such sites have been also recently proposed [15], where it was found that spectral bands in the blue and VNIR part of the spectrum are the most appropriate for detection of OOMW using multispectral satellite datasets. The index and other image analysis techniques were applied also in very high resolution satellite data [16].

In this study, an attempt to detect OOMW disposal areas automatically or semi-automatically with minimum feedback from end-users is presented. For this purpose, the paper aims to investigate the applicability of high resolution data that is freely distributed to end-users. The paper examines the contribution of high resolution satellite images provided from Google Earth (GE) as well as archived GeoEye OrbView-3 images in order to detect OOMW disposal areas.

A critical aspect of the use of GE is the parameter of scale (*i.e.* height of observation) as well the accuracy of the results. Therefore, the paper aims to identify the optimum scale of GE images for the detection of OOMW for the area of Crete. To date, a very limited number of studies have been conducted to map OOMW from free available images such as GE. GE has been widely used by scholars for detection of objects and targets using innovative algorithms as well for mapping land use and land use changes with a great success [23–25].

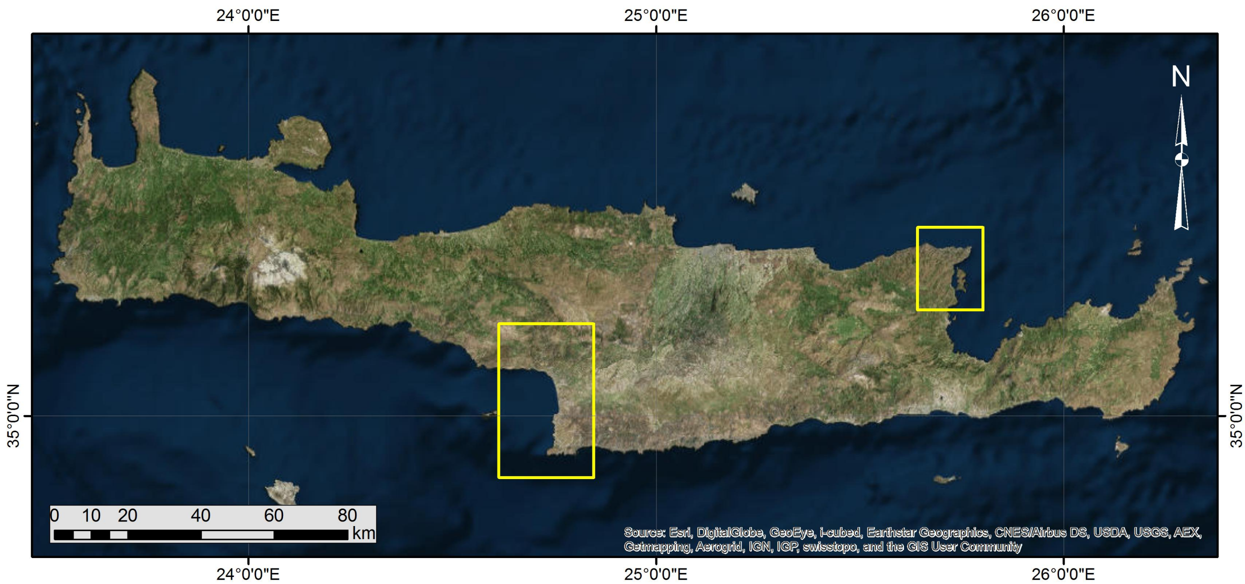

Figure 1: The two areas of interest on the island of Crete (indicated with yellow colour).

2 Study Areas

The area of olive groves in Greece has increased constantly during the last quarter of the century, as a result of planting of new high-density groves, reaching an area of about 8.336 km^2 in 2007 (+120.000 ha since 1991) [14]. Olive groves have expanded in many semi-mountainous and coastal areas, mainly in Crete and Peloponnese [26]. Greece ranks third worldwide in terms of olive oil production while the island of Crete contributes approximately 5% to the total world olive oil production [11].

In Crete, as in any other areas that produce olives, the olive-oil mill wastes are normally deposited at tanks, or directly in the soil or even on adjacent torrents, rivers and lakes posing a high risk to the environmental pollution and the community health. In these cases, the main environmental problems stem from the very high values in oxygen requirement, large concentrations of toxic compounds affecting the ecosystems and human health [27]. Long-term disposal of waste, without the necessary monitoring and protective measures, can cause changes in the physicochemical parameters of the territory with the risk of future non-tissue degradation of the environment. Moreover, older waste sites often lack reliable geological or artificial barriers and depositional information to minimize the possibilities of causing further environmental damages to the soil and groundwater. The problem of environmental contamination and waste management is one of the main concerns of earth scientists and responsible local authorities in other related fields of science around the globe [28]

For the purpose of this paper, two areas of interest have been selected (Figure 1). The first area (case study 1: Mesaras inlet) is located in the southern-central part of Crete while the second area (case study 2: Mironikitas area) is situated in the northeastern part of Crete. In these areas typical OOMW disposal areas are found since olive trees are cultivated by local people. In both areas, field observations have been also performed by the authors in the last years (after 2011).

3 Resources and Methodology

3.1 Case study 1: Mesaras inlet

For the first case study located in the Mesaras inlet, a GeoEye's OrbView-3 image was used. GeoEye's OrbView-3 satellite was able to provide high-resolution imagery from space. OrbView-3 collected one meter panchromatic or four meter multispectral (NIR-R-G-B) imagery at a swath width of 8 km. The U.S. Geological Survey (USGS) Earth Resources Observation and Science (EROS Center) received 179,981 OrbView-3 image "segment" from GeoEye with no restrictions. The data were delivered in Basic Enhanced (Level 1B) radiometric corrected format. The product files include satellite telemetry data, rational functions, post-processed Ground Sample Distance (GSD) at nadir data, and sufficient metadata for rigorous triangulation. The data in this collection were acquired between September 2003 and March 2007, from the multispectral (MS) and panchromatic (PAN) sensors. More than 84% of Orbview-3 collection re PAN images [29]. The detailed methodology followed in this case study was to automatically identify OOMW disposal areas by performing the following seven (7) steps:

Step 1 (Orthorectification). Initially the high resolution GeoEye OrbView-3 satellite (overpass 18 June 2006) was orthorectified using the Rational Polynomial Coefficients (RPC) file and the ASTER Global Digital Elevation Model (ASTER GDEM) data available for this area. The orthorectification was applied to minimize distortions of the image caused by topography, camera geometry, and other sensor-related errors. The RPC file was generated from ephemeris data while the ASTER GDEM data was downloaded from Earth Remote Sensing Data Analysis Center (ERSDAC) website.

Step 2 (Pan-Sharpening). This step was applied in order to improve the spatial resolution of the multispectral bands of the OrbView-3 image. Pan-sharpening techniques have been widely used in remote sensing applications to improve the quality of the multispectral images [30]. The Brovey transformation was applied to improve the spatial resolution of the multispectral image, as it is one of the simpler but more widely-used RGB colour fusion techniques [31] due to its high degree of spatial enhancement, speed, and ease of implementation. The basic procedure is to first multiply each multispectral band by the high-resolution panchromatic band, and then divide each product by the sum of the multispespectral bands [32]. The PAN band of the GeoEye OrbView-3 with spatial resolution of 1 m was merged with the multispectral bands of the same sensor with 4 m spatial resolution.

Step 3 (SAM target detection). The next step was the application of the SAM for OOMW target detection [33]. SAM is based on the idea that an observed reflectance spectrum can be considered as a vector in the multidimensional space. To compare two different spectra (*e.g.* pixels), the angle between these two vectors is calculated. If the angle is smaller than a given tolerance level, the spectra is considered to match [33]. SAM algorithm was found to be the most promising (*i.e.* less candidates pixels classified as OOMW disposal areas) compared to other known algorithms applied also for this study, such as Matched Filtering; Constrained Energy Minimization; Adaptive Coherence Estimator etc. A small (Region Of Interest) ROI was selected from a known OOMW disposal site while other non-OOMW ROIs were also selected to improve the quality of the results. Special attention was given to select representative ROIs for OOMW disposal areas as well other similar targets that may produce false positives. A critical parameter was the SAM maximum angle field, to define which pixel may (or may not) be classified as OOMW areas. Based on the spectral profiles from in-situ observations [34], it was found that OOMW disposal areas tend to have low reflectance values in the visible part of the spectrum ($\rho < 5\%$) and relative high reflectance values in the near infrared part of the spectrum ($\rho = 10\%$). Thus, a minimum SAM angle was decided using these thresholds.

Step 4 (Filtering (sieving and clumping)). In spite of SAMs high performance, a significant number of false pixels within the image classified as OOMW areas will still remain. For this reason, a threshold and filtering of the image was necessary. Both mode and clumping filtering were applied to the removal of 2 pixels in order to remove any noise and group isolated pixel together. This procedure is similar with the "salt and pepper" effect [34] which appeared after pixel based classifications of satellite data. Mode filtering was applied to solve the problem of isolated pixels occurring in the classified images (*i.e.* less than 2 pixels). Using the clumping filtering, similar classified areas were grouped together using morphological operators and therefore minimizing isolated pixels.

Step 5 (Masking using topographical parameters). Using the ASTER GDEM dataset, the slope of the case study area was calculated in the ArcGIS v10 environment. Following, areas with a slope of more than 20% (hilly areas) were excluded (masked) from the analysis since OOMW disposal areas were found to be located either on flat or almost flat regions in the island of Crete.

Step 6 (Querying image using geometric properties). The areas and lengths of the groups of pixels were calculated using a GIS. A SQL query was then applied based on specific geometric and shape properties (*i.e.* length more than 10meters; area larger than 50 square meters) in order to further exclude false areas. The SQL parameters were based on the field observations carried out by the authors in several OOMW disposal areas.

Step 7 (Accuracy assessment). The final step for this semi-automatic approach assessed the accuracy of the results by comparing the detected OOMW disposal areas with known OOMW areas of the region.

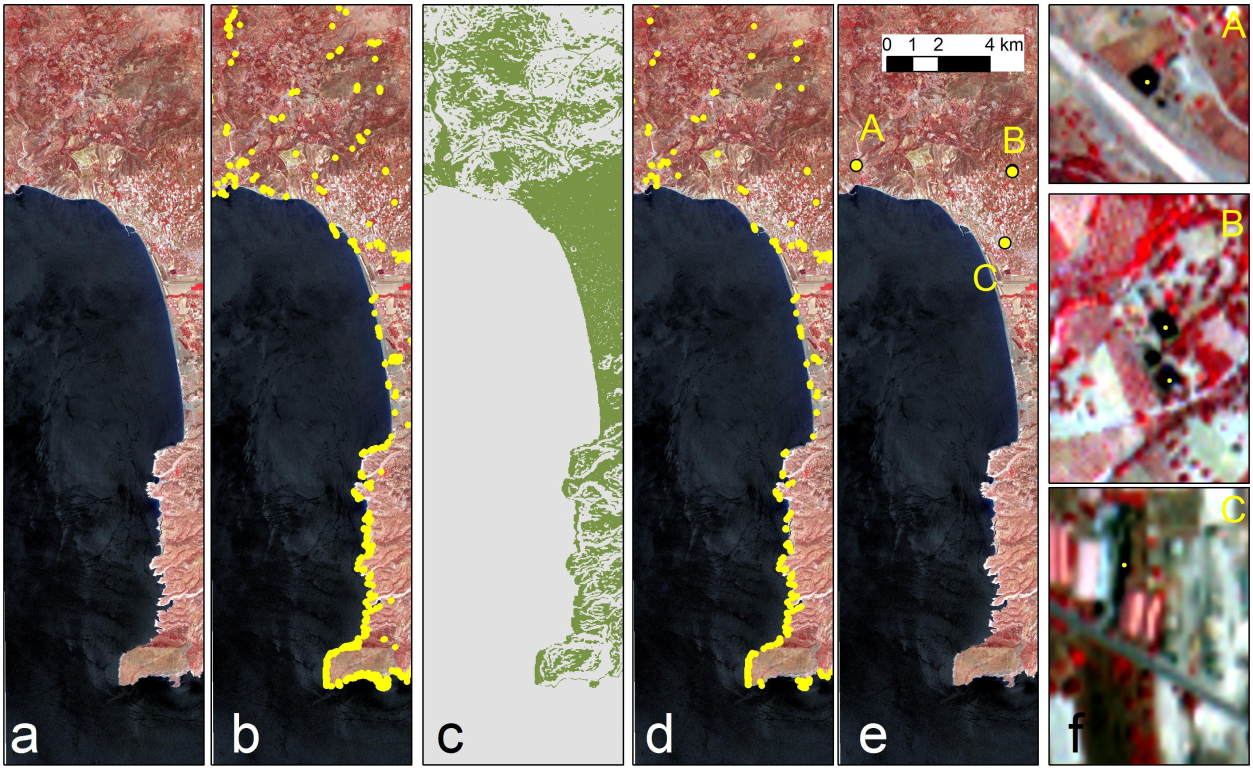

Figure 2: (a) The semi-automatic identification of OOMW disposal areas in the area of Mesaras inlet for the different steps of the applied methodology: Initially the orthorectification of the image was performed, and then; **(b)** the SAM detection algorithm was applied. Yellow pixels indicate the candidate areas as OOMW disposal areas; Then **(c-d)** the results were masked based on topographic parameters (slope >20%) while the final stage; **(e)** involved the extraction of OOMW sites based on geometric properties. The final four areas as detected from the methodology applied in the Mesaras area are shown in the last column **(f)**.

3.2 Case study area 2: Mironikitas area

In the second case study, GE images were evaluated. GE releases free images at high spatial resolution that can potentially be used for regional land use/cover mapping as well for the detection of objects in inaccessible sites. GE provides very high resolution (VHR) natural-colour (red-green-blue, RGB) images based on commercial space borne sensors. In spite of the limitations that GE images have, including compression of the original satellite images, loss of image quality and no NIR band is provided, it is noted that several researchers have demonstrated the great potential of GE (and similar digital globes) to support research and to provide updated information [35–37].

While interpretation of these free distributed high resolution images can be accurate enough, this approach is very time-consuming and automatic procedures will be of great value. A variety of well-known classification algorithms such as Minimum Distance (MD); Maximum Likelihood (ML); Mahalanobis Distance; Spectral Angle Mapper (SAM) as well Support Vector Machine (SVM) were evaluated for the Mironikitas area. OOMW disposal areas, vegetation, soil and water were classes used for the classification procedure. A number of random pixels within the different images were used to train as well evaluate the final results. Moreover, different scales of GE images were evaluated in order to examine the impact of scale on classification accuracy (*i.e.* detection of OOMW disposal areas).

4 Results

4.1 Case study area 1: Mesaras inlet

As shown in Figure 2, after the application of SAM detection algorithm (Step 3), a small number of false positives still remain (≈ 0.03% of the initial dataset). Coastal and shadow areas were found to include false positives. To improve the results, a topographic restriction was applied under the ArcGIS environment (Step 5). The slope of the region was calculated based on the ASTER GDEM data. Since OOMW waste disposal areas are found in mainly flat or almost flat regions, a threshold of slope = 20% was used (Figure 2, c and d) to mask the results from the SAM detection algorithm (Figure 2).

More than 50% of the initial areas were eliminated in this manner. The final step was to apply geometrical queries to the remaining target areas. Simple geometrical and shape features were used to exclude either very small or very large regions (based on the area), or to ignore targets based on the length of the feature. Shape properties (*e.g.* area to length parameter) were also applied to exclude non-rectangular areas. The parameter for both shape as well length properties is based upon in-situ knowledge related to the local practices on the island. The queries were applied using the ArcGIS v10 environment. The final results (Figure 2f) show that the remaining areas are limited to four potential OOMW disposal areas.

From field campaigns carried out by the authors since 2011, only one OOMW disposal area (Figure 2f; Point A) was cross validate with the results from the automatic detection using the GeoEye OrbView-3. Field photos from this OOMW disposal area (*i.e. Agia Galini*) are shown in Figure 3. These sites along with the database developed for OOMW areas in Crete [11] have been used as ground truth data.

Closer inspection of the other three OOMW disposal areas (Figure 2f; B-C) based on archive satellite images from GE and personal communication with the local people of the area have confirmed that the OOMW disposal areas have been correctly identified from the entire GeoEye OrbView-3 image. Therefore the methodology applied to GeoEye OrbView-3 was able not only to detect known OOMW disposal areas but at the same time to uncover old areas (*i.e.* not currently used as disposal areas). Taking this into consideration, archive satellite data may reveal additional OOMW sites as well, which are undetected and probably not recorded by in-situ observations. Such OOMW areas have dimensions of almost 30 × 30 meters while variations in the size can be also observed.

Figure 3: Photos from the Agia Galini OOMW disposal area taken in 2011. This OOMW corresponds to the result of Figure 2f; Point A.

4.2 Case study area 2: Mironikitas area

For the second case study area in the region of Mironikita, GE images were used. In this area, three OOMW disposal areas have been identified from field observations carried out by the authors. The purpose for this case study was to evaluate the potential use of detection of OOMW areas using RGB images from GE. Several classification techniques were evaluated. In the literature different supervised and unsupervised classification techniques exist, *e.g.* per-pixel based maximum likelihood (ML), nearest neighbor, fuzzy classifications, object-oriented multi-resolution segmentation, artificial neural networks, decision tree-based classification, and rule-based classification [34, 37–41]. Using areas of interest, the overall performance of each technique can be measured and evaluated based on statistical analyses.

The MD algorithm is a statistical technique that classifies the image based on the closest distance of training areas using the spectral characteristics of the pixels [33]. It is possible to specify a maximum distance threshold; *i.e.*, if the distance is still further away than that threshold, it is assumed that none of the groups are similar enough and the result will be "unknown" the ML algorithm performs classification based on the normal probability density function [39]. The SAM algorithm is an automated method which calculates and classifies the spectral angle between the pixels of the image [39]. SVM is a machine-learning technique that is well adapted to solving non-linear, high dimensional space classifications. SVM can be used for remote sensing applications, for classification of either multispectral or hyperspectral data, in which there

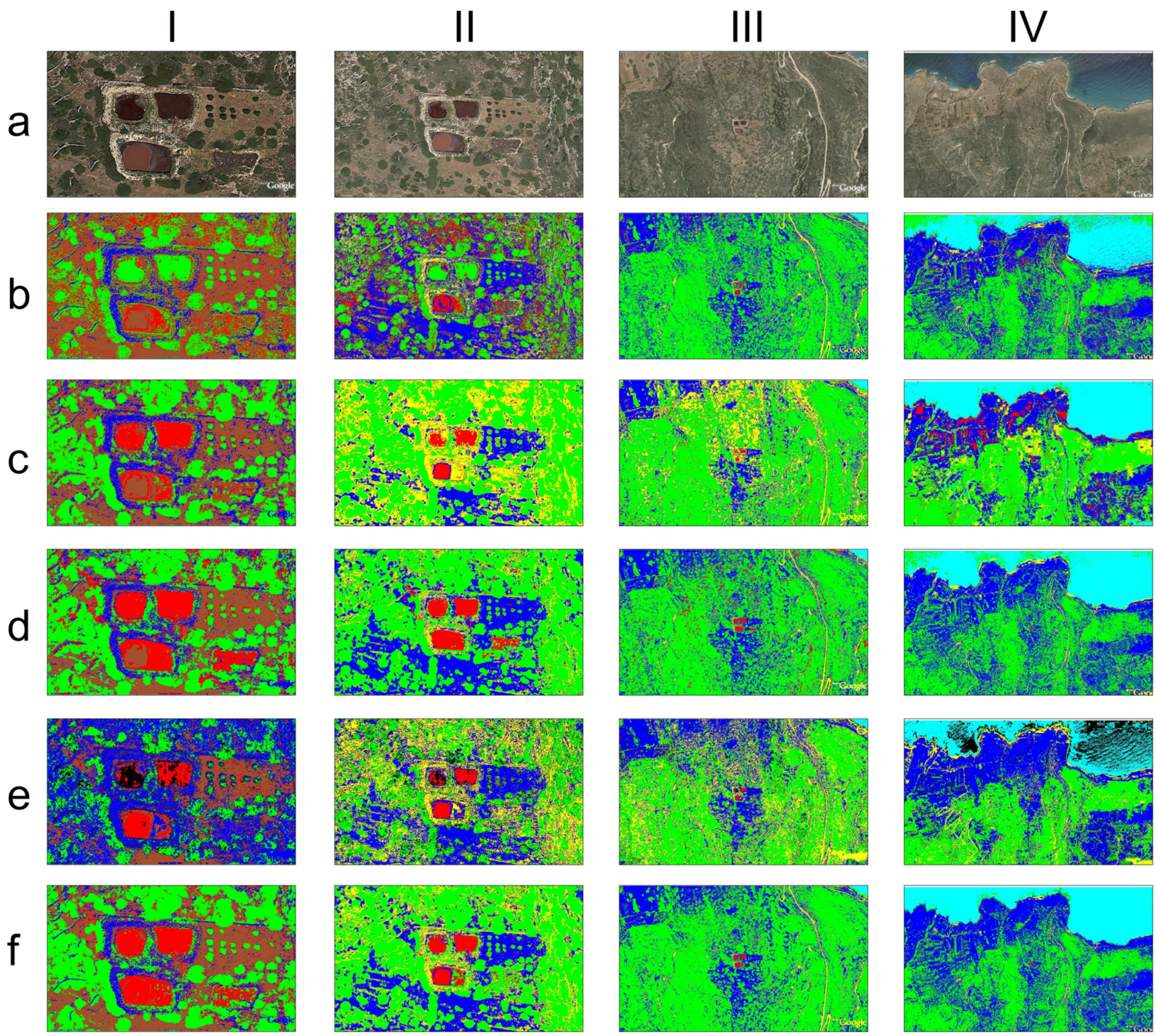

Figure 4: Classification results for the Mironikita area in four different scales (I-IV: 100; 250; 850 and 2000 meters above the OOMW area respectively). Row **(a)** corresponds to GE image; **(b)** for MD classification; **(c)** ML classification; **(d)** Mahalanobis classification; **(e)** SAM classification and **(f)** SVM classification results. Red shades indicate the OOMW areas; brown and blue shades represent soil while green areas are vegetated.

is a spectral similarity between the pixels [42]. SVM aims to identify the boundaries between classes in n-dimensional spectral-space [43]. According to [44], SVM classifiers have been shown to attain high accuracies in land cover mapping and outperform other algorithms.

Four different observation heights were selected as shown in Figure 4. Figure 4a was captured from a height of approximately 100 meters above the OOMW area while Figure 4b was captured from a height of 250 meters. Figure 4c was exported from a height of 850 meters while Figure 4d represents a height of approximately 2000 meters over the same area. Red shades indicate the OOMW areas; brown and blue represents soil while green areas are vegetated. The classifications results (*i.e.* Kappa coefficient; overall accuracy; producer accuracy and user accuracy) for each case are shown in Table 1.

For the classification procedure, ROIs from the GE images were selected to train the corresponding classifier into three main categories: OOMW disposal areas; soil and vegetation. In addition, other ROIs were also selected from the images for validation purposes. The ROIs were selected based on interpretation of the images as well as from existing knowledge of the area from previous field visits. It should be also noticed that the same ROIs were used for

Table 1: Kappa coefficient; overall accuracy; producer accuracy and user accuracy for the classification results at four different scales using different classifiers at the Mironikita area: 100 m; 250 m; 850 m and 2000 m.

Observation height	Classifier (Kappa Coefficient)					Classifier (Overall Accuracy)				
	MD	ML	Mahal.	SAM	SVM	MD	ML	Mahal.	SAM	SVM
100	0.33	0.66	0.81	0.53	0.92	0.55	0.77	0.86	0.66	0.93
250	0.41	0.91	0.92	0.65	0.86	0.52	0.92	0.92	0.76	0.92
850	0.70	0.96	0.95	0.65	0.91	0.76	0.92	0.93	0.73	0.92
2000	0.69	0.74	0.77	0.69	0.82	0.73	0.74	0.84	0.82	0.89
Observation height	**Classifier (Producer's Accuracy)**					**Classifier (User's Accuracy)**				
	MD	ML	Mahal.	SAM	SVM	MD	ML	Mahal.	SAM	SVM
100	26.25	60.92	83.44	53.92	93.44	61.25	86.97	90.94	74.91	93.12
250	42.07	78.91	92.47	69.66	82.93	40.84	89.60	91.91	79.25	91.33
850	61.44	96.21	95.69	62.40	87.11	87.01	92.36	92.83	89.54	94.36
2000	48.21	88.56	72.17	54.37	85.00	79.41	75.28	87.26	80.65	87.81

all classifiers for all images, while the same ROIs were applied for validation for all the different scales. This was performed so as to represent as well as possible representative results from Mironikita area, thereby minimizing any bias. Finally, ROIs for the OOMW disposal areas have been collected only from a single OOMW pond.

Accuracy assessment has been a topic of considerable debate and research in remote sensing for many years. This is in part because the promoted standard methods such as the Kappa coefficient are not always appropriate [45]. Several researchers have worked on the problems relative to accuracy assessment of classification uncertainty [46–48]. This paper provides established accuracy measures for OOMW areas. As shown in Figure 4 and Table 1, classification accuracy is not directly related to the scale of the image. In fact, as seen in Figure 4a (MD classifier), the OOMW area was more accurately classified at the lower scale (Figure 4b-4c, MD classifier). This is also the case for the other classifiers. Several studies showed that the optimal spatial resolution is not necessarily associated with the highest spatial resolution satellite imagery [48]. This is generally the case in heterogeneous areas (such as OOMW areas) where the optimal pixel size is influenced by the spatial structure of the investigated objects and the image processing designs, *e.g.*, spectral classification, regression, texture analysis [49]. As [**?**] pointed out, an appropriate scale for observation is a function of the type of environment and the kind of information desired. The choice of scale is therefore determined by the size of the studied area and the type of phenomena analysed.

The SVM classifier provided the best overall performance and stability for detecting the OOMW areas, regardless of the scale of the image. In contrast, MD tend to give poor results at all scales (Kappa coefficient < 0.70) while SAM classification provides better results when the image was captured at a higher elevation (see Table 1). In contrast, ML classification tends to give poor results at small and large scales (Figures 4a – 4d). The results show that the optimum viewing height for the majority of the classifications is from heights of 850 meters (see Table 1), suggesting that this height can also be used in other areas to classify (and therefore detect) OOMW areas from GE images.

5 Discussion

The exposure of unknown OOMW disposal areas highlights the advantage of remote sensing images for the detection of current waste disposal areas, as well as old waste disposal areas which have been contaminated from olive oil waste. The identification of such areas is also important for local authorities in order to take the necessary measures to minimize any pollution of the soil. As it was shown from the results, remote sensing data and image analysis can be used by local stakeholders to systematic monitor and control OOMW areas.

An integrated system for local authorities can be developed where GIS systems integrated with satellite datasets and semi-automatic procedures can be efficiently used to detect and monitor OOMW areas. Satellite data, either freely distributed as shown in this study, or high and very high resolution images can be used so as to detect automatically OOMW areas. In addition, 3D digital globes such as Google Earth©, Bing Map© etc. can also support the GIS system since they can provide usefully information as well as historical datasets. Ground spectroradiometers and geophysical surveys can be also used for monitoring OOMW areas. Such ground technologies may be used so as to further optimize the system and the GIS procedures [15, 31] and to examine underground pollution. The system will be able to record in a 4D space (X,Y,Z and time) the OOMW areas for the island of Crete.

6 Conclusions

The olive oil industry is very important in Mediterranean countries, with Greece being the 3rd largest olive oil producers worldwide. The extraction of olive oil generates huge quantities of waste, which can be harmful for the environment. In Greece, more than 1000 OOMW disposal areas have been recorded. These OOMW disposal areas are scattered all over the island and their detection and mapping might be difficult and time consuming if done by using in-situ surveys observations.

Olive oil mill wastes constitute a major factor in pollution in olive-growing regions and an important problem to be solved for the agricultural industry in Greece. The main reasons are: a) the huge waste production in a relatively short time, which should, ideally, be processed and deposited safely to the environment before the next production period. b) the physicochemical characteristics of these wastes, some of which can cause a significant degradation of the subsurface c) the very high organic load of the wastes and some inorganic materials (compounds of nitrogen and phosphorus, sodium, potassium, iron, etc.) while, although not toxic, the high and repetitive concentration on the surface (disposal sites) can cause serious environmental problems. Studies have shown changes in the physicochemical parameters of soils both within the landfills and the surrounding area [3, 4, 28]. The long-term olive oil mills waste deposition can lead to future serious degradation of soil and groundwater quality. The purpose of this research is to propose holistic and integrated methods for identifying, monitoring and addressing environmental degradation that takes place in areas of waste disposal sites.

Alternative ways are needed to detect as well as to monitor OOMW areas. Remote sensing techniques offer a cost-effective solution for detecting OOMW disposal areas. In this paper, freely distributed, high resolution satellite images were evaluated in two different cases studies. In the first case study a GeoEye OrbView-3 image was used to semi-automatically detect potential OOMW sites. The detection was based on the SAM classifier followed by topographical and geometrical queries to improve the results. The results were found to be very promising, given that three new OOMW areas were detected in the region with coverage of approximately 240 square kilometres, while the fourth OOMW disposal area of *Agia Galini* (Figure 3) has confirmed the image results.

The proposed methodology implemented in this paper indicates that remote sensing data freely distributed can be efficiently used so as to record and monitor OOMW sites in vast areas. Such approach can be used for local stakeholders to control such disposal areas even in areas where access is difficult. Other remote sensing technologies, such as ground geophysical surveys, can be also used in an integrated system so as to monitor the underground pollution related with OOMW diposal areas. Further work is expected to be carried out by the authors in the near future using high resolution and very high resolution satellite datasets as well as the use of radar images. Sensitivity analysis can be also applied in the future so as to optimize even further the methodology (*e.g.* thresholds values). Radiometric and atmospheric conditions can alter the final results; therefore, radiometric calibration is necessary. If this step is ignored, then thresholds values (SAM angle) should be maximized.

Acknowledgement: This work was performed in the framework of the PEFYKA project within the KRIPIS Action of the General Secretariat for Research and Technology (GSRT). The project is funded by Greece and the European Regional Development Fund of the European Union under the NSRF and the O.P. Competitiveness and Entrepreneurship.

References

[1] Asfi M., Ouzounidou G., Panajiotidis S., Therios I., Moustakas M. Toxicity effects of olive-mill wastewater on growth, photosynthesis and pollen morphology of spinach plants. Ecotoxicology and Environmental Safety, 2012, 80(1), 69–75.

[2] Roig A., Cayuela M.L., Sánchez-Monedero M.A. An overview on olive mill wastes and their valorisation methods. Waste Management, 2006, 26(9), 960–969.

[3] Doula M. Strategies to improve and protect soil quality from the disposal of olive oil mills' wastes in the Mediterranean region PROSODOL. Final Report, LIFE Project Number LIFE07 ENV/GR/000280, 2013.

[4] Rodis P.S., Karathanos V.T., Mantzavinou A. Partitioning of olive oil antioxidants between oil and water phases. Journal of Agricultural and Food Chemistry, 2002, 50, 596–601.

[5] Paredes M.J., Moreno E., Ramos-Cormenzana A., Martinez J. Characteristics of soil after pollution with wastewaters from olive oil extraction plants. Chemosphere, 1987, 16 (7), 1557–

1564.
[6] Dellagreca, M., Monaco, P., Pinto, G., Pollio, A., Previtera, L., Temussi F. Phytotoxicity of low-molecular-weight phenols from olive mill wastewaters. Bulletin of Environmental Contamination and Toxicology, 2001, 67, 352–359.
[7] Niaounakis M., Halvadakis C. P. Olive processing waste management. Literature review and patent survey. Waste Management Series, 2006, ISBN: 978-0-08-044851-0.
[8] Karydas C.G., Sekuloska T., Sarakiotis I. Use of imagery to indicate landscape features important when assessing environmental risk caused by olive farming and olive oil production. IASME/WSEAS International Conference onnEnergy, Environment, Ecosystems and Sustainable Development, 2005, Athens, Polytechnic School of Athens.
[9] Karydas C.G., Manakos I., Sarakiotis I., Sekuloska T. Minimum dataset for risk management of water pollution caused by olive oil factories in Crete. 25th EARSeL Symposium, Porto - Portugal, 2005, 267–275.
[10] Ntougias S., Gaitis F., Katsaris P., Skoulika S., Iliopoulos N., Zervakis I.Z. The effects of olives harvest period and production year on olive mill wastewater properties – Evaluation of Pleurotus strains as bioindicators of the effluent's toxicity. Chemosphere, 2013, 92(4), 399–405.
[11] Alexakis D. D., Sarris A., Papadopoulos N., Soupios P., Doula M., Cavvadias V. GEODIAMETRIS: An integrated geoinformatic approach for monitoring land pollution from the disposal of olive oil mill wastes. Proc. SPIE 9229, Second International Conference on Remote Sensing and Geoinformation of the Environment (RSCy2014), 92291L, 2014, doi:10.1117/12.2066335.
[12] Simyrdanis, K.; Papadopoulos, N.; Kirkou, S.; Sarris, A.; Tsourlos, P. Monitoring of olive oil mills' wastes using electrical resistivity tomography techniques. Proc. SPIE 9229, Second International Conference on Remote Sensing and Geoinformation of the Environment (RSCy2014), 92291P, 2014; doi: 10.1117/12.2066298.
[13] Myint S.W., Yuan M., Cerveny R.S., Giri C.P. Comparison of Remote Sensing Image Processing Techniques to Identify Tornado Damage Areas from Landsat TM Data. Sensors 2008, 8, 1128–1156.
[14] Alexakis D.D., Sarris A., Kalaitzidis C., Papadopoulos N., Soupios P. Integrated use of satellite remote sensing, GIS and ground spectroscopy techniques for monitoring olive oil mill waste disposal areas in Crete Island –Greece. International Journal of Remote Sensing, 2016, 37(3), 669–693.
[15] Agapiou A., Papadopoulos N., Sarris A. Discriminant analysis of olive oil mill wastes using spectroradiometers in the visible and near infrared part of the spectrum, European Journal of Remote Sensing, 2015, 48, 793-809, doi: 10.5721/EuJRS20154844.
[16] Agapiou A., Papadopoulos N., Sarris A. Monitoring olive mills waste disposal areas in Crete using very high resolution satellite data, The Egyptian Journal of Remote Sensing and Space Sciences, 2016, 19(2), 285–295
[17] Karydas C. G., Sekuloska T., Sarakiotis I. Use of EO data to identify landscape features associated to assessment of environmental risk caused by olive farming and olive oil production. In: Proceedings (CD) of the IASME/WSEAS International Conference on Energy, Environment, Ecosystems and Sustainable Development, Athens, Greece (July), 2005.
[18] Silvestri S., Omri M. A method for the remote sensing identification of uncontrolled landfills: formulation and validation. International Journal of Remote Sensing, 2008, 29(4), 975–989.
[19] Slonecker T., Fisher G.B., Aiello D.P., Haack, B. Visible and Infrared Remote Imaging of Hazardous Waste: A Review. Remote Sening, 2010, 2, 2474–2508.
[20] Giancarlo B., Silvestri S., Gobbo L., Furlan E., Valenti S., Rosselli R. GIS, multi-criteria and multi-factor spatial analysis for the probability assessment of the existence of illegal landfills. International Journal of Geographical Information Science, 2009, 23(10), 1233–1244.
[21] Kwarteng A. Y., Al-Enezi A. Assessment of Kuwait's Al-Qurain Landfill Using Remotely Sensed Data. Journal of Environmental Science and Health Part A: Toxic/Hazardous Substances and Environmental Engineering 2004, 39(2), 351–364, DOI: 10.1081/ESE-120027527.
[22] Dewidar K. M. Landfill detection in Hurghada North Red Sea, Egypt, using Thematic Mapper images. International Journal of Remote Sensing, 2002, 23(5), 939–948.
[23] Ghaffarian S., Ghaffarian S. Automatic building detection based on Purposive FastICA (PFICA) algorithm using monocular high resolution Google Earth images. ISPRS Journal of Photogrammetry and Remote Sensing, 2014, 97, 152–159.
[24] Jacobson A., Dhanota J., Godfrey J., Jacobson H., Rossman Z., Stanish A., Walker H., Riggio J. A novel approach to mapping land conversion using Google Earth with an application to East Africa. Environmental Modelling & Software, 2015, 72, 1–9.
[25] Johansen K., Phinn S., Taylor M. Mapping woody vegetation clearing in Queensland, Australia from Landsat imagery using the Google Earth Engine. Remote Sensing Applications: Society and Environment, 2015, 1, 36–49.
[26] Kavvadias V., Doula M.K., Komnitsas K., Liakopoulou N. Disposal of olive oil mill wastes in evaporation ponds: Effects on soil properties. Journal of Hazardous Materials, 2010, 182, 144–155.
[27] Camarsa G., Gardner S., Jones W., Eldridge J., Hudson T. Thorpe E., Hara E. Good practice in improving environmental performance in the olive oil sector. Luxembourg: Office for Official Publications of the European Union. 2010.
[28] PROSODOL: "Strategies to improve and protect soil quality from the disposal of Olive Oil Mill Wastes in the Mediterranean region: Results and Achievements of a 4-year demonstration project - What to consider; What to do", M. K. Doula V. Kavvadias K. Komnitsas Federico Tinivella Luis Moreno Ortego Apostolos Sarris (Eds) 2012, LIFE07 ENV/GR/000280. USGS, 2014. OrbView-3. https://lta.cr.usgs.gov/satellite_orbview3 (last accessed May 2015).
[29] Zhang Y. Understanding image fusion. Photogrammetric Engineering & Remote Sensing, 2004, 70(6), 657–661.
[30] Nikolakopoulos G. K. Comparison of nine fusion techniques for very high resolution data. Photogrammetric Engineering & Remote Sensing 2008, 74(5), 647–659.
[31] Agapiou A., Papadopoulos N., Sarris A. Building spectral libraries for monitoring olive mill wastewater (OMW) disposal areas, SafeChania 2015: The Knowledge Triangle in the Civil Protection Service, 10-12 June 2015, Chania, Greece.
[32] Garzelli A., Nencini F. Panchromatic sharpening of remote sensing images using a multiscale Kalman filter. Pattern Recognition, 2007, 40(12), 3568–3577.
[33] Lillesand T. M., Kiefer R. W., Chipman J. Remote Sensing and Image Interpretation, Lehigh Press, 7th Edition, ISBN: 978-1-118-91947-7, 2015.

[34] Chan H. R., HoC.-W., Nikolova M. Salt-and-Pepper Noise Removal by Median-Type Noise Detectors and Detail-Preserving Regularization. IEEE Transactions on image processing, 2005, 14(10), 1479–1485.
[35] Ghaffarian S., Ghaffarian S. Automatic building detection based on Purposive FastICA (PFICA) algorithm using monocular high resolution Google Earth images. ISPRS Journal of Photogrammetry and Remote Sensing, 2014, 97, 152–159.
[36] Kennedy D., Bishop M.C. Google earth and the archaeology of Saudi Arabia. A case study from the Jeddah area. Journal of Archaeological Science, 2011, 38(6), 1284–1293.
[37] Blaschke T. Object based image analysis for remote sensing. ISPRS Journal of Photogrammetry and Remote Sensing, 2010, 65(1), 2–16.
[38] Campbell J. B., Wynne R. H. Introduction to Remote Sensing, The Guilford Press, New York, 5th Edition, 2011.
[39] Jensen J. R. Introductory Digital Image Processing: A Remote Sensing Perspective Prentice Hall, 4th Edition, 2015, ISBN-13: 978-0134058160.
[40] Mountrakis G., Im J., Ogole C. Support vector machines in remote sensing: A review. ISPRS Journal of Photogrammetry and Remote Sensing, 2011, 66 (3), 247–259.
[41] Heumann B.W. An object-based classification of mangroves using a hybrid decision tree Support Vector Machine approach. Remote Sensing, 2011, 3, 2440–2460.
[42] Yuhendra A. I., Sumantyo S.T.J., Kuze H. Assessment of pan-sharpening methods applied to image fusion of remotely sensed multi-band data. International Journal of Applied Earth Observation and Geoinformation, 2012, 18165–175, 10.1016/j.jag.2012.01.013.
[43] Paneque-Gálvez J., Mas J.-F., Moré G., Cristóbal J., ORTA-Martínez M., Luz C.A., Guèze M. Macía J. M., Reyes-García V. Enhanced land use/cover classification of heterogeneous tropical landscapes using support vector machines and textural homogeneity. International Journal of Applied Earth Observation and Geoinformation, 2013, 23, 372–383.
[44] Foody M. G. Status of land cover classification accuracy assessment. Remote Sensing of Environment, 2002, 80, 185–201.
[45] Liu C., Frazier P., Kumar. L. Comparative assessment of the measures of thematic classification accuracy. Remote Sensing of Environment, 2007, 107, 606–616.
[46] Olofsson P., Foody M. D., Stehman V. S., Woodcock E. C. Making better use of accuracy data in land change studies: Estimating accuracy and area and quantifying uncertainty using stratified estimation. Remote Sensing of Environment, 2013, 129, 122–131.
[47] Olofsson P., Foody M. D., Stehman V. S., Woodcock E. C., Wulder M. A. Good practices for estimating area and assessing accuracy of land change. Remote Sensing of Environment, 2014, 148, 42–57.
[48] Woodcock C.E., Strahler A.H. The factor scale in remote sensing. Remote Sensing of Environment 1987, 21, 311–332.
[49] Tran T.-B., Puissant A., Badariotti D., Weber C. Optimizing Spatial Resolution of Imagery for Urban Form Detection – The Cases of France and Vietnam. Remote Sensing, 2011, 3(10), 2128–2147.